Insulator-metal transition induced by interlayer coupling in $La_{0.6}Sr_{0.4}MnO_3/SrTiO_3$ superlattices

M. Izumi,* Y. Ogimoto, Y. Okimoto, and T. Manako
Joint Research Center for Atom Technology (JRCAT), Tsukuba 305-0046, Japan

P. Ahmet, K. Nakajima, and T. Chikyow†
National Institute for Research in Inorganic Materials, Tsukuba 305-0044, Japan

M. Kawasaki
Joint Research Center for Atom Technology (JRCAT), Tsukuba 305-0046, Japan
and Department of Innovative and Engineered Materials, Tokyo Institute of Technology, Yokohama 226-8502, Japan

Y. Tokura
Joint Research Center for Atom Technology (JRCAT), Tsukuba 305-0046, Japan
and Department of Applied Physics, University of Tokyo, Tokyo 113-8656, Japan
(Received 26 December 2000; revised manuscript received 14 May 2001; published 24 July 2001)

The electronic and magnetic properties of perovskite superlattices composed of five unit-cell layers of ferromagnetic metal $La_{0.6}Sr_{0.4}MnO_3$ and nonmagnetic band insulator $SrTiO_3$ with varying layer thickness have been systematically investigated. The superlattices have well-defined periodic stacking with no sign of interlayer diffusion. The spin canting at the interfaces in $La_{0.6}Sr_{0.4}MnO_3$ layers manifests itself as a suppressed magnetization and huge magnetoresistance subsisting to low temperature. The transport properties show a clear crossover from insulating to metallic perhaps by an increase in the interlayer electron hopping through $SrTiO_3$ layers when the $SrTiO_3$ layer thickness is reduced. This crossover is also discerned in the infrared optical spectra as the filling of absorption in the low-energy region.

DOI: 10.1103/PhysRevB.64.064429 PACS number(s): 75.30.Vn, 75.70.−i, 75.70.Cn

I. INTRODUCTION

Perovskite manganese oxides have recently been attracting great interest because of intriguing magnetoelectronic phenomena such as gigantic magnetoresistance, charge-orbital ordering, metal-insulator transitions, etc.[1] The interplay among charge, spin, and orbital degrees of freedom plays a crucial role in realizing various ground states in such a correlated electron system. Among them, $La_{1-x}Sr_xMnO_3$ (LSMO), having the highest Curie temperature (T_C) ~ 370 K (at $x=0.4$) among the manganites, has been extensively studied.[2] Since the density of states at the Fermi level (E_F) in LSMO is occupied almost by the majority-spin electrons alone in the ferromagnetic (FM) and metallic states,[3] attempts have been made to use this almost 100% spin polarization in the form of heterostructures such as tunnel junctions.[4] However, a far inferior performance to that expected implies the importance of interface issues. For example, the LSMO($x=1/3$)/$SrTiO_3$/LSMO($x=1/3$) tunnel junction shows a fairly large tunneling magnetoresistance at low temperatures as expected, but it disappears around 200 K.[5] Since the magnetization is almost saturated at 200 K ($\sim T_C/2$), large magnetoresistance should be present at this temperature. The unexpected suppression of magnetoresistance well below T_C has also been reported in other literature.[6] We suspect that a sort of modulation of ferromagnetism such as spin canting takes place in LSMO adjacent to $SrTiO_3$ (STO). By using superlattices containing many interfaces of interest, such a spin canting effect can be quantitatively studied by measurements of magnetization and transport properties,[7] since the double-exchange mechanism in metallic conductance is sensitive to spin-state modification.[8]

Until now, several groups have reported on LSMO/STO or $La_{1-x}Ca_xMnO_3$/STO superlattices,[9] in which the suppression both in T_C and magnetization was observed as the thickness of Mn oxide layers decreases. This has been attributed to the deformation of the crystal structure of Mn oxide layers in the superlattices. In fact, lattice strain in these compounds

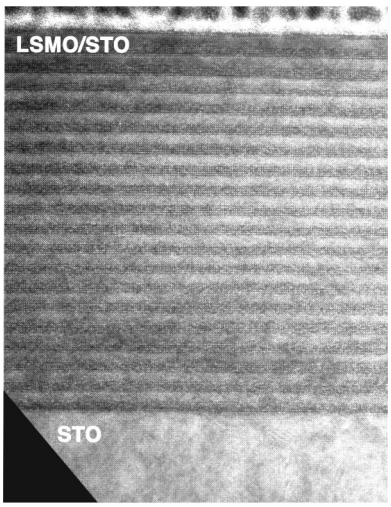

FIG. 1. An HRTEM image of a [$La_{0.6}Sr_{0.4}MnO_3$ 5 u.c./$SrTiO_3$ 5 u.c.] superlattice along the [100] axis. Dark and bright areas indicate $La_{0.6}Sr_{0.4}MnO_3$ and $SrTiO_3$ layers, respectively.

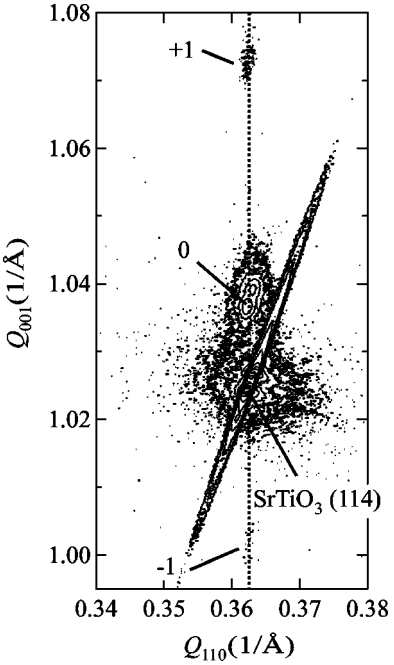

FIG. 2. An x-ray diffraction contour mapping in the reciprocal space around the perovskite (114) peak for a [$La_{0.6}Sr_{0.4}MnO_3$ 5 u.c./$SrTiO_3$ 4 u.c.] superlattice. The abscissa and the ordinate indicate the position of reciprocal lattice along the [110] and [001] directions, respectively. The superlattice satellite peaks are denoted as -1 and $+1$.

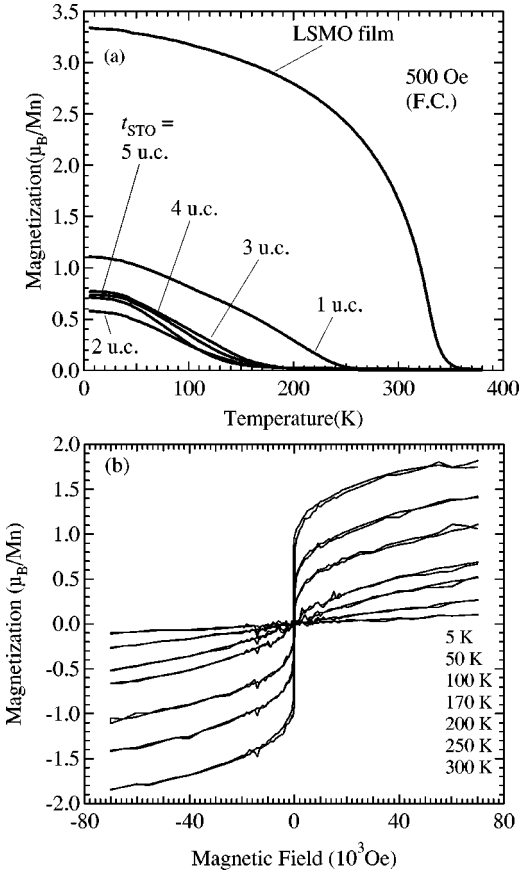

FIG. 3. (a) Temperature dependence of magnetization for [LSMO 5 u.c./STO t_{STO}] superlattices. Magnetization was measured during warming in a magnetic field of 500 Oe applied along [100] in the film plane. Magnetization is normalized by the $La_{0.6}Sr_{0.4}MnO_3$ layer thickness. (b) Magnetization of the [$La_{0.6}Sr_{0.4}MnO_3$ 5 u.c./$SrTiO_3$ 2 u.c.] superlattice as a function of magnetic field. Each *M-H* curve is measured after zero-field cooling at 7 T. There is no difference between the magnetization after field cooling and zero-field cooling. Magnetization is not saturated even at a temperature far lower than T_C ($=170$ K).

can give a huge effect on the electronic properties through the orbital-lattice coupling channel.[10,11] Therefore, quantitative and careful studies are needed to investigate the spin-structure modification inherent in the interface region. In this study, the effects of spin canting in LSMO and possible electron hopping across STO layers on the electronic properties of superlattices are clearly demonstrated by ruling out the strain effect through detailed structural characterization.

II. EXPERIMENT

LSMO($x=0.4$)/STO superlattices were grown by a pulsed laser deposition method as reported previously with controlling the layer thickness by the intensity oscillation of reflection high-energy electron diffraction.[7,12] Single crystals of STO with an atomically flattened (001) surface ($a=b=c=0.391$ nm) were used as the substrates.[13] An LSMO 100-nm single-layer film was also fabricated for comparison. X-ray diffraction (XRD) measurements were performed with a four-circle goniometer. A sample for high-resolution transmission electron microscopy (HRTEM) was prepared by a focused-ion-beam microsampling technique with use of 30-kV accelerated Ga ions. The HRTEM observation was operated at 400 kV. Magnetic measurements were carried out by a superconducting quantum interference device magnetometer. Resistivity with magnetic field up to 7 T applied along the film plane was measured by a conventional four-probe method. In the optical measurements, transmittance [$T(\omega)$] and reflectivity [$R(\omega)$] spectra were measured using a Fourier-transform-type spectrometer ($0.2<\hbar\omega<0.8$ eV) and grating monochrometer ($0.6<\hbar\omega<3.0$ eV). The absorption coefficient [$\alpha(\omega)$] was calculated by the relation $\alpha(\omega)=-\ln\{T(\omega)/[1-R(\omega)]\}/d$, d being the total thickness of LSMO layers.

III. RESULTS AND DISCUSSION

The LSMO layer thickness was fixed at 5 unit cells (u.c.) throughout this study and the STO layer thickness (t_{STO}) was varied from 1 to 5 u.c. Superlattices are represented as [LSMO 5 u.c./STO t_{STO}] in this paper. We denote the crystal indices in the tetragonal unit cell setting the c axis perpendicular to the film plane. The HRTEM image in Fig. 1 shows a clear contrast between LSMO and STO due to compositional modulation along the stacking direction. The interfaces are flat and aligned evenly as we expected. Detailed analyses of the interface structure based on chemical lattice imaging indicated no or minimal, if any, interlayer atomic diffusion.[14] Figure 2 shows a typical contour mapping in the reciprocal space obtained by an XRD measurement for [LSMO 5 u.c./

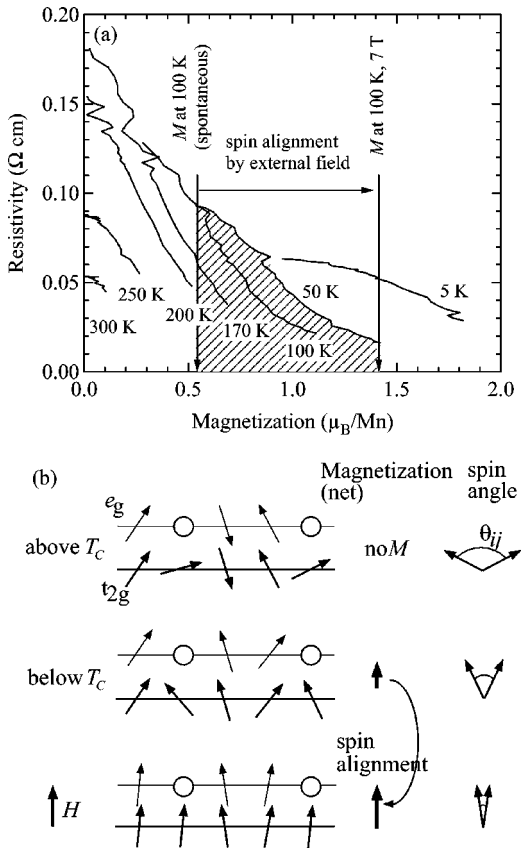

FIG. 4. (a) Resistivity for a [LSMO 5 u.c./STO 2 u.c.] superlattice as a function of magnetization observed in the *M-H* curve. To avoid the domain rotation component in the magnetoresistance at a small magnetic field, data in the range of 0.05 T$<H<$7 T are used. (b) Schematic illustration of the relationship between the magnetization and resistivity. Below T_C, spins show long-range order, with some canting configuration. The local (t_{2g}) spins are further aligned toward the collinear spin configuration by applying an external magnetic field, resulting in an enhanced mobility of conduction electrons.

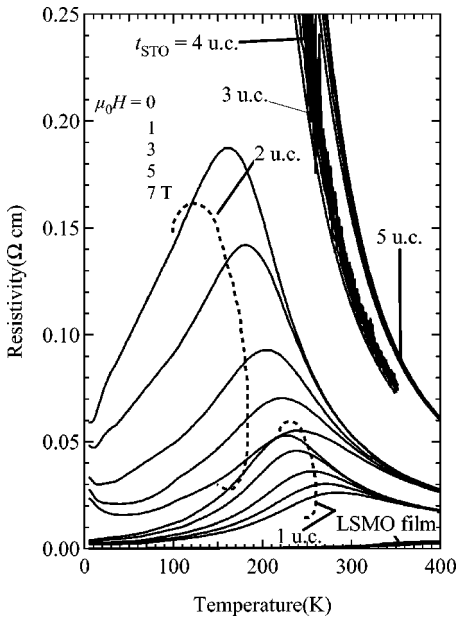

FIG. 5. Temperature dependence of resistivity for [LSMO 5 u.c./STO t_{STO}] superlattices at various magnetic fields. Only the total thickness of $La_{0.6}Sr_{0.4}MnO_3$ layers was used to calculate ρ for the superlattices. The resistivity was measured during warming after field cooling. The data for the $La_{0.6}Sr_{0.4}MnO_3$ single-layer film are also shown for comparison.

STO 4 u.c.]. The peaks arising from the superlattice (denoted as 0, ± 1) have identical Q_{110} values to that of the substrate peak, indicating that the crystal symmetry is deformed into a tetragonal symmetry with $a=b=0.391$ nm to match the in-plane lattice constant of the substrate. Such a lattice deformation was observed for all samples investigated here, being consistent with the fact that there can scarcely be seen a misfit dislocation in the HRTEM picture. Thus, we can rule out a change in the crystal structure as a source of any change in the electronic and magnetic properties of superlattices having various layer thickness because all the films are equally subject to the biaxial tensile strain.

Figure 3 shows the magnetization of superlattices with various t_{STO} as a function of temperature and magnetic field. The magnetization is normalized by the volume of the LSMO layer. In Fig. 3(a), a significant reduction can be seen both in the magnitude of magnetization and T_C compared with the single-layer film. The T_C of 140 K and the spontaneous magnetization of $0.86\mu_B$/Mn for [LSMO 5 u.c./STO 5 u.c.] are significantly reduced from those for the single-layer film, 338 K and $3.42\mu_B$/Mn, respectively. Figure 3(b) shows the *M-H* curves of [LSMO 5 u.c./STO 2 u.c.] at the various temperatures. The magnetization increases gradually with increasing magnetic field even above 5×10^4 Oe, indicating the presence of spin canting.

In the scheme of a double-exchange interaction,[8] the resistivity can be related to the magnitude of magnetization. In this model, the electron hopping interaction between neighboring Mn sites is proportional to $\cos(\theta_{ij}/2)$, θ_{ij} being the angle between the neighboring Mn local (t_{2g} electron) spins. To elucidate the transport and spin structure quantitatively, we plot in Fig. 4 the relationship between the resistivity and magnetization of [LSMO 5 u.c./STO 2 u.c.]. As clearly seen, the resistivity is decreased with the magnetization induced by an external magnetic field. Below $T_C=170$ K, where long-range magnetic correlation develops, finite spontaneous magnetization arises, and correspondingly the resistivity already decreases. However, application of a magnetic field of 7 T further increases the magnetization from $0.55\mu_B$/Mn to $1.4\mu_B$/Mn at 50 K, shown as the hatched area in Fig 4(a). In accordance with increasing the magnetization (reducing the θ_{ij}) by applying 7 T, the resistivity is monotonically decreased to about 1/5. Thus, we can conclude that the magnetic field changes the canted spin alignment, which perhaps arises from the interface with STO layers, toward the FM collinear spin one, and as a result, the electron hopping between the adjacent Mn sites is largely enhanced.

Since the counter STO layer bears almost no spins that can destabilize the ferromagnetism of LSMO, a mechanism other than spin frustration at the interface[7,15] must be considered as the origin of spin canting. The most plausible origin

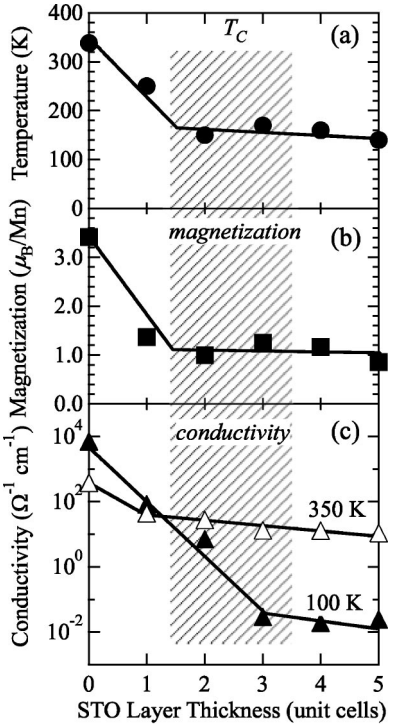

FIG. 6. (a) Ferromagnetic transition temperature T_C, (b) spontaneous magnetization at 5 K, and (c) conductivity on a logarithmic scale at 100 K (solid symbols, below T_C) and 350 K (open symbols, above T_C) as a function of $SrTiO_3$ layer thickness (t_{STO}). The conductivity changes significantly in the hatched area with changing $SrTiO_3$ layer thickness in spite of the almost constant values of T_C and magnetic moment.

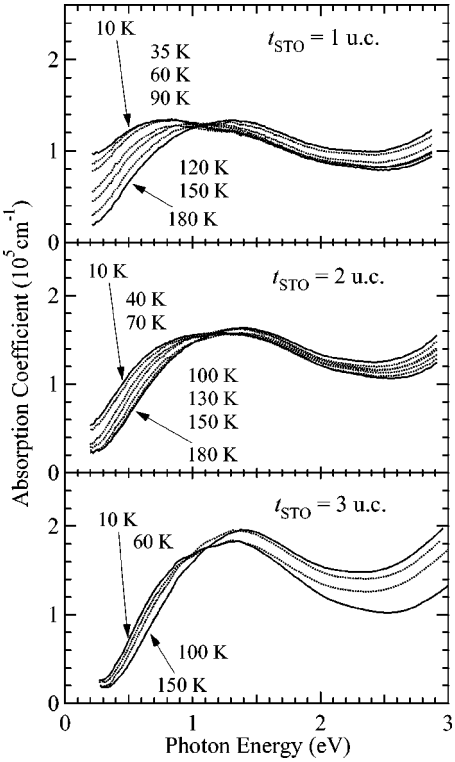

FIG. 7. Variation of the absorption spectra for the $La_{0.6}Sr_{0.4}MnO_3/SrTiO_3$ superlattices at various temperatures below T_C. The $SrTiO_3$ layer thickness (t_{STO}) is varied from one to three unit cells.

is a gradual change from an FM to a layer-type antiferromagnetic (AF) state at the vicinity of the interface. The AF phase is often observed in heavily doped Mn oxide perovskites.[16] In the case of LSMO, a layer-type AF state appears for $x > 0.5$ in bulk samples,[17] and in thin films tensile lattice strain from the substrate expands the layer-type AF region to a lower-doping region.[11] This is because a small c/a value splits the degenerate e_g energy level into lower-lying x^2-y^2 and higher-lying $3z^2$-r^2 levels, and the increase of occupancy in the x^2-y^2 orbital induces the layer-type AF spin ordering.[16] In this context, the LSMO $x=0.4$ film with tensile strain is positioned near the boundary between the double-exchange FM and superexchange AF phasess. Therefore, if even a small amount of charge transfer occurs between LSMO and STO through the interface, the marginal FM ordering in LSMO may be easily destabilized. For instance, hole injection from STO to LSMO is likely caused by interruption of the periodic sequence of the $La_{0.6}Sr_{0.4}O$ sheet in LSMO by the SrO sheet in $SrTiO_3$ at the interface. Some other mechanisms might also affect the magnetism of LSMO cooperatively or competitively.

Figure 5 shows the in-plane resistivity as a function of temperature. The superlattices show a clear insulator-to-metal transition as t_{STO} is reduced from 3 to 2 u.c. The enhancement of the resistivity (ρ) with an increase of t_{STO} as well as the large magnetoresistance subsisting down to the lowest temperature for superlattices with $t_{STO} \leqslant 2$ can be partly explained by the double-exchange model taking account of spin canting.[8] It is known that FM ordering within the *ab* plane and AF coupling along the *c* direction are realized in the *metallic* layer-type AF phase of $Nd_{0.45}Sr_{0.55}MnO_3$.[18] Therefore, metallic conductivity is still expected in the present superlattices as well because of electron conduction within the FM plane. Actually, even though the magnetization is as small as about 17–33 % of the fully FM LSMO thick film, reflecting the almost layer-type AF state, metallic conduction appears for [LSMO 5 u.c./STO 1 u.c.] and [LSMO 5 u.c./STO 2 u.c.]. In this sense, the magnetoresistance of [LSMO 5 u.c./STO 2 u.c.] shown in Fig. 4 is partly ascribed to the field-driven FM alignment between neighboring MnO_2 sheets.[18] However, we need an additional carrier-localization mechanism in the superlattices to account for such a large change in ρ or the metal-insulator transition as a function of t_{STO}. The spin canting near the interface induces the confinement of the double-exchange carriers into the narrowed width of the LSMO layer. Such an effective reduction in the electronic dimension may cause another instability, leading to carrier localization, such as charge ordering.

To clarify the relation between the magnetic and transport properties, we plot T_C, spontaneous magnetization, and conductivity ($\sigma \equiv 1/\rho$) as a function of t_{STO} in Fig. 6. With an increase of t_{STO}, σ decreases drastically at both 350 K ($>T_C$) and 100 K ($<T_C$) as seen in Fig. 6(c). There is a crossover region (hatched area) where only σ decreases with the magnetization and T_C being kept nearly constant. In this

region, σ at 100 K decreases by more than two orders of magnitude with an increase of the STO layer only by 1 u.c. Since the magnetization of the superlattice changes little in this region, this abrupt change in σ should be attributed not to the change in spin canting, but to that of the charge dynamics affected by the electronic coupling between adjacent LSMO layers separated by STO.

To probe the variation of electronic structure with t_{STO}, we measured the optical spectra in an infrared-to-visible region (0.2–3.0 eV). Figure 7 shows the absorption spectra $[\alpha(\omega)]$ of the superlattices with $t_{STO}=1,2$, and 3 u.c. The $\alpha(\omega)$ steeply decreases toward $\hbar\omega=0$ eV regardless of the temperature for [LSMO 5 u.c./STO 3 u.c.], indicating the presence of a charge gap (Δ) of 0.2–0.3 eV, which is comparable to a typical value of the charge-ordered manganite $Pr_{0.6}Ca_{0.4}MnO_3$ ($\Delta=0.18$ eV).[19] On the other hand, the $\alpha(\omega)$ for [LSMO 5 u.c./STO 1 u.c.] develops in the low-energy region with decreasing temperature, which is consistent with the metallic temperature dependence of ρ. At the intermediate t_{STO} of 2 u.c., a small but finite $\alpha(\omega)$ is discerned in a low-energy region below T_C ($\sim$150 K). The observed systematic change of optical spectra suggests that the electronic structure of the superlattice is modified over a fairly large energy region (0–1 eV) by change of t_{STO} from 1 to 3 u.c. The interlayer electron hopping such as carrier tunneling through STO barrier layers appears to suppress Δ, which would be otherwise developed in the 5-u.c.-thick LSMO single layer. When $t_{STO}\geqslant 3$ u.c., the interlayer electron hopping is so small that the carriers are confined within ultrathin (5 u.c.) LSMO layers with considerable spin canting.

On the basis of these spectral features, we speculate that some kind of charge ordering within the thin LSMO layer is induced to develop such a large Δ. In particular, the checkerboard-type charge ordering accompanying breathing-type Mn- O bond distortion is likely present in the insulating $x=0.4$ layer of the superlattice, where the nearly-layer-type AF state is realized with $d_{x^2-y^2}$ orbital ordering. In fact, the possibility of such a charge ordering has been extensively argued theoretically[20,21] and experimentally[22] for the layer-type AF phase of $x\sim 0.5$ doped manganites. As t_{STO} is reduced to less than 2 u.c., the electron hopping or hybridization effect through STO layers contributes to the recovery of conductivity perhaps via the melting of charge ordering although the spin-canted region is still preserved.

IV. CONCLUSION

The presence of spin canting in LSMO at the interface was evidenced by the transport and magnetic properties of LSMO (5 u.c.)/STO superlattices. Since the in-plane lattice constant of the films is identical to that of the $SrTiO_3$ substrate, the strain effect can be ruled out as a source of any modification in physical properties with a change of $SrTiO_3$ layer thickness. A crossover from an insulating to a metallic state occurs when the STO layer thickness is reduced from 3 to 2 u.c. Optical spectra of the superlattices show the presence of a fairly large charge gap, being reminiscent of the charge ordering instability inherent to two-dimensionally confined electron systems. The charge gap is observed to be closed in the course of the dimensional crossover with a decrease of the STO layer thickness.

ACKNOWLEDGMENT

This work was partly supported by the New Energy and Industrial Technology Development Organization (NEDO).

*Present address: Research Center for Advanced Science and Technology, The University of Tokyo, Tokyo 153-8904, Japan.

†On leave from National Research Institute for Metals, Tsukuba, 305-0047, Japan.

[1] For late advances, see, for example, M. Imada, A. Fujimori, and Y. Tokura, Rev. Mod. Phys. **70**, 1039 (1998); Y. Tokura and N. Nagaosa, Science **288**, 21 (2000).

[2] A. Urushibara, Y. Moritomo, T. Arima, A. Asamitsu, G. Kido, and Y. Tokura, Phys. Rev. B **51**, 14 103 (1995).

[3] J.-H. Park, E. Vescovo, H.-J. Kim, C. Kwon, R. Ramesh, and T. Venkatesan, Nature (London) **392**, 794 (1998).

[4] V.A. Vas'ko, V.A. Larkin, P.A. Kraus, K.R. Nikolaev, D.E. Grupp, C.A. Nordman, and A.M. Goldman, Phys. Rev. Lett. **78**, 1134 (1997); J.M. De Teresa, A. Barthélémy, A. Fert, J.P. Contour, R. Lyonnet, F. Montaigne, P. Seneor, and A. Vaurès, *ibid.* **82**, 4288 (1999); D.C. Worledge and T.H. Geballe, Appl. Phys. Lett. **76**, 900 (2000).

[5] J.Z. Sun, W.J. Gallgher, P.R. Duncombe, L. Krusin-Elbaum, R.A. Altman, A. Gupta, Yu Lu, G.Q. Gong, and Gang Xiao, Appl. Phys. Lett. **69**, 3266 (1996); Yu Lu, X.W. Li, G.Q. Gong, Gang Xiao, A. Gupta, P. Lecoeur, J.Z. Sun, Y.Y. Wang, and V.P. Dravid, Phys. Rev. B **54**, R8357 (1996).

[6] T. Obata, T. Manako, Y. Shimakawa, and Y. Kubo, Appl. Phys. Lett. **74**, 290 (1999); J. O'Donnell, A.E. Andrus, S. Oh, E.V. Colla, and J.N. Eckstein, *ibid.* **76**, 1914 (2000); Moon-Ho Jo, N.D. Mathur, N.K. Todd, and M.G. Blamire, Phys. Rev. B **61**, R14 905 (2000).

[7] M. Izumi, Y. Murakami, Y. Konishi, T. Manako, M. Kawasaki, and Y. Tokura, Phys. Rev. B **60**, 1211 (1999); M. Izumi, T. Manako, Y. Konishi, M. Kawasaki, and Y. Tokura, *ibid.* **61**, 12 187 (2000).

[8] P.W. Anderson and H. Hasegawa, Phys. Rev. **100**, 675 (1955).

[9] C. Kwon, K.-C. Kim, M.C. Robson, J.Y. Gu, M. Rajewswari, T. Venkatesan, and R. Ramesh, J. Appl. Phys. **81**, 4950 (1997); H. Tabata, K. Ueda, Y. Muraoka, and T. Kawai, Trans. Mater. Res. Soc. Jpn. **24**, 13 (1999); M.-H. Jo, M.N. Mathur, J.E. Evetts, M. Blamire, M. Bibe, and J. Fontcuberta, Appl. Phys. Lett. **75**, 3689 (1999).

[10] A.J. Millis, T. Darling, and A. Migliori, J. Appl. Phys. **83**, 1588 (1998); Y. Suzuki, H.Y. Hwang, S-W. Cheong, and R.B. van Dover, Appl. Phys. Lett. **71**, 140 (1997); F. Tsui, M.C. Smoak, T.K. Nath, and C.B. Eom, *ibid.* **76**, 2421 (2000).

[11] Y. Konishi, Z. Fang, M. Izumi, T. Manako, M. Kasai, H. Kuwahara, M. Kawasaki, K. Terakura, and Y. Tokura, J. Phys. Soc. Jpn. **68**, 3790 (1999); Z. Fang, I.V. Solovyev, and K. Terakura, Phys. Rev. Lett. **84**, 3169 (2000).

[12] M. Izumi, Y. Konishi, T. Nishihara, S. Hayashi, M. Shinohara, M. Kawasaki, and Y. Tokura, Appl. Phys. Lett. **73**, 2497 (1998).

[13] M. Kawasaki, K. Takahashi, T. Maeda, R. Tsuchiya, M. Shino-

hara, T. Yonezawa, O. Ishihara, M. Yoshimoto, and H. Koinuma, Science **266**, 1540 (1994).
[14] T. Chikyow *et al.* (unpublished).
[15] I. Panagiotopoulos, C. Christides, M. Pissas, and D. Niarchos, Phys. Rev. B **60**, 485 (1999); H. Tanaka and T. Kawai, Solid State Commun. **112**, 201 (1999).
[16] R. Maezono, S. Ishihara, and N. Nagaosa, Phys. Rev. B **57**, R13 993 (1998); **58**, 11 583 (1998), and references therein.
[17] H. Fujishiro, M. Ikebe, and Y. Konno, J. Phys. Soc. Jpn. **67**, 1799 (1998).
[18] H. Kuwahara, T. Okuda, Y. Tomioka, A. Asamitsu, and Y. Tokura, Phys. Rev. Lett. **82**, 4316 (1999).
[19] Y. Okimoto, Y. Tomioka, Y. Onose, Y. Otsuka, and Y. Tokura, Phys. Rev. B **57**, R9377 (1998); **59**, 7401 (1999).
[20] T. Mizokawa and A. Fujimori, Phys. Rev. B **56**, R493 (1997); T. Mizokawa, D.I. Khomskii, and G.A. Sawatzky, *ibid.* **63**, 024403 (2001).
[21] F. Mack and P. Horsch, Phys. Rev. Lett. **82**, 3160 (1999).
[22] T. Ishikawa, K. Tobe, T. Kimura, T. Katsufuji, and Y. Tokura, Phys. Rev. B **62**, 12 354 (2000).